Available online at www.sciencedirect.com
SCIENCE DIRECT®
Polyhedron 24 (2005) 1710–1716
POLYHEDRON
www.elsevier.com/locate/poly

Syntheses, spectral and structural studies of Schiff base complexes of η^5-pentamethylcyclopentadienyl rhodium and iridium

Padavattan Govindaswamy [a], Yurij A. Mozharivskyj [b], Mohan Rao Kollipara [a,*]

[a] Department of Chemistry, North-Eastern Hill University, Shillong 793 022, India
[b] Ames Laboratory, Iowa State University of Science and Technology, Ames, Iowa, IA 50011, USA

Received 6 April 2005; accepted 27 April 2005
Available online 14 July 2005

Abstract

The compounds $[(\eta^5\text{-}C_5Me_5)M(\mu\text{-}Cl)Cl\}_2]$ where M = Rh (**1**) and Ir (**2**) react with *N*,*N*′-donor chelating ligands, viz., *para*-substituted *N*-(pyrid-2-ylmethylene)phenylamines (**2-PP**) in methanol–acetone to afford the pentamethylcyclopentadienyl rhodium (III) and iridium (III) derivatives of the type $[(\eta^5\text{-}C_5Me_5)MCl(C_5H_4N\text{-}2\text{-}CH{=}N\text{–}C_6H_4\text{-}p\text{-}X]^+$ (M = Rh, **3**; M = Ir, **4**), where C_5Me_5 = pentamethylcyclopentadienyl; X = H (**3a**, **4a**), CH_3 (**3b**, **4b**), OCH_3 (**3c**, **4c**), Cl (**3d**, **4d**), NO_2 (**3e**, **4e**), respectively. These compounds were characterized by FT-IR and FT-NMR spectroscopy as well as analytical data. The molecular structures of the tetrafluoroborate salt of $[(\eta^5\text{-}C_5Me_5)RhCl(C_5H_4N\text{-}2\text{-}CH{=}N\text{–}C_6H_4\text{-}p\text{-}Cl)]^+$ (**3d**) and hexafluorophosphate salt of $[(\eta^5\text{-}C_5Me_5)IrCl(C_5H_4N\text{-}2\text{-}CH{=}N\text{–}C_6H_4\text{-}p\text{-}NO_2)]^+$ (**4e**) were established by single crystal X-ray diffraction studies.

Keywords: Pentamethylcyclopentadienyl; *N*,*N*′-chelating ligands; Pyridine-2-carboxaldehyde; Rhodium and iridium complexes

1. Introduction

Half-sandwich complexes have proved to be extremely useful in stoichiometric and catalytic asymmetric synthesis and have therefore attracted much study [1–5]. In addition, their four-coordinate pseudo-tetrahedral geometry makes them particularly suitable for investigation of the stereochemistry of reactions at the metal centre [6]. Many studies of cyclopentadienyl and arene ruthenium (II) complexes with bidentate ligands have shown that substitution reactions occur predominantly with retention of configuration at the metal [7]. Until recently far fewer studies had been carried out on pentamethylcyclopentadienyl rhodium (III) and iridium (III) complexes with chelating *N*,*N*′-donor bases.

We had reported previously the syntheses of arene and cyclopentadienyl ruthenium complexes containing *N*,*N*′-donor Schiff base ligands derived from pyridine-2-carboxaldehyde [8]. We had also communicated syntheses of cyclopentadienyl–ruthenium (II) [9], indenyl–ruthenium (II) [10], cyclopentadienyl–osmium (II) and arene–ruthenium (II) [11] complexes with a variety of nitrogen-based ligands. However, the analogous pentamethylcyclopentadienyl–rhodium (III) and iridium (III) Schiff base complexes have not been explored as much as the corresponding cyclopentadienyl and arene ruthenium (II) complexes [12]. As a part of our continuing study, we would like to report herein the syntheses and characterization of new cationic pentamethylcyclopentadienyl rhodium (III) and iridium (III) complexes with *N*,*N*′-donor Schiff base ligands, viz., various *para*-substituted *N*-(pyrid-2-ylmethylene)phenylamines (**2-PP**). The molecular structures of representative compounds are solved by X-ray crystallography and are reported as well.

* Corresponding author. Tel.: +91 364 272 2620; fax: +91 364 255 0076.
E-mail addresses: kmrao@nehu.ac.in, mrkollipara@yahoo.com (M.R. Kollipara).

0277-5387/$ - see front matter © 2005 Elsevier Ltd. All rights reserved.
doi:10.1016/j.poly.2005.04.034

2. Experimental

2.1. Physical measurements

Elemental analyses were performed on a Perkin–Elmer-2400 CHN/O analyzer. Infrared spectra were recorded on a Perkin–Elmer Model 983 spectrophotometer with the sample prepared as KBr pellets. Electronic spectra were recorded on a Hitachi-300 spectrophotometer. The ^{1}H NMR and ^{13}C{^{1}H} NMR spectra were recorded in acetone-d_6 and $CDCl_3$ solvents with TMS as internal standard and recorded on a Bruker ACF-300 (300 MHz) spectrometer, the coupling constants J being given in Hz. Electro-chemical studies (in acetonitrile) were performed with a PARC electrochemistry system as described elsewhere [13]. In cyclic voltametry (CV) the following parameters were used, namely, the scan rate 100 mV s^{-1} and the formal potential $E^0 = 0.5(E_{pa} + E_{pc})$, where E_{pa} and E_{pc} are the anodic and cathodic peak potentials, respectively; and ΔE_p is the peak-to-peak separation.

2.2. Materials and methods

All chemicals used were of reagent grade. All reactions were carried out in distilled and dried solvents. Rhodium chloride and iridium chloride were purchased from Arora Matthey Ltd., and used as received. Pyridine 2-carboxaldehyde (Fluka) was used as received. All liquid aromatic amines were reagent grade and were distilled prior to use, while solid aromatic amines were used as such. The ligands C_5H_4N-2-CH=NC_6H_4-*p*-X (where X = H, CH_3, OCH_3, Cl, NO_2) [14], and the precursor complexes [{(η^5-C_5Me_5)M(μ-Cl)Cl}$_2$] (where M = Rh (**1**) and Ir (**2**)) [15] were prepared by known literature methods. The purification of acetonitrile and the preparation of tetrabutylammonium perchlorate [Bu$^n_4$N][ClO_4], used as solvent and supporting electrolyte, respectively, in the electrochemical experiments, were performed following a literature method [16].

2.3. Synthesis of [(η^5-C_5Me_5)RhCl(C_5H_5N-2-CH=NC_6H_4-*p*-X)]$^+$ (**3a-e**), (X = H (**3a**), CH_3 (**3b**), OCH_3 (**3c**), Cl (**3d**), NO_2 (**3e**))

The following general procedure was used for the preparation of these five complexes:

Method 1: A mixture of the starting complex [{(η^5-C_5Me_5)Rh(μ-Cl)Cl}$_2$] (**1**) (100 mg, 0.110 mmol), the appropriate Schiff base ligand **2-PP** (0.242 mmol) and NH_4PF_6 (0.242 mmol) was stirred in methanol–acetone (20/10 v/v mixture) for 6 h until the color of the solution changed from red to orange. The solvent was removed in vacuo, the residue dissolved in dichloromethane (5 ml), and the solution filtered to remove ammonium chloride. The orange solution was concentrated to 2 ml, when addition of excess hexane gave the orange-yellow complex, which was separated and dried under vacuum.

Method 2: A mixture of the complex [{(η^5-C_5Me_5)Rh(μ-Cl)Cl}$_2$] (**1**) (100 mg, 0.110 mmol), the ligand **2-PP** (0.242 mmol) and NH_4PF_6 (0.242 mmol) was stirred in methanol (20 ml) for a few hours, whereupon the orange-yellow product separated out. The orange-yellow product was centrifuged, washed with diethyl ether and dried under vacuum.

3a. Yield: 152 mg, (78%). IR (KBr pellets, cm^{-1}): $\nu_{(C=N)}$ 1593 (s), $\nu_{(P-F)}$ 844 (s).

^{1}H NMR ($CDCl_3$ and acetone-d_6, δ): 1.56 (s, 15H, C_5Me_5), 7.32–7.56 (m, 3H, Ph), 7.64 (d, 2H, J_{H-H} = 6.53 Hz, Ph), 8.03–8.55 (m, 3H, py), 8.97 (d, 1H, J_{H-H} = 4.86 Hz, py), 9.24 (s, 1H, imine C–H).

^{13}C NMR (acetone-d_6, δ): 7.60 (CH_3, C_5Me_5), 97.53 (C, C_5Me_5), 122.44, 129.43, 129.79, 131.36 (Ph), 140.34, 148.80, 152.66, 154.04, 155.32 (py), 166.97 (C–H).

Elemental *Anal.* Calc. for $C_{22}H_{25}RhN_2ClPF_6$: C, 43.98; H, 4.19; N, 4.66. Found: C, 43.65; H, 4.02; N, 4.71%.

UV–Vis (acetone): λ_{max} = 359.6 nm.

3b. Yield: 159 mg, (80%). IR (KBr pellets, cm^{-1}): $\nu_{(C=N)}$ 1596 (m), $\nu_{(P-F)}$ 844 (s).

^{1}H NMR ($CDCl_3$ and acetone-d_6, δ): 1.52 (s, 15H, C_5Me_5), 2.44 (s, 3H, CH_3), 7.35 (d, 2H, J_{H-H} = 2.31 Hz), 7.67 (d, 2H, J_{H-H} = 8.22 Hz), 7.83–7.87 (dd, 1H, J_{H-H} = 3.96 Hz), 8.20 (d, 2H, J_{H-H} = 4.22 Hz), 8.57 (d, 1H, J_{H-H} = 2.81 Hz), 8.89 (d, 2H, J_{H-H} = 5.36 Hz).

^{13}C NMR (acetone-d_6, δ): 7.63 (CH_3, C_5Me_5), 18.34 (CH_3), 98.37 (C, C_5Me_5), 112.24, 115.62, 116.96, 122.32 (Ph), 123.37, 126.21, 128.56, 131.34, 145.36 (py), 158.56 (C–H).

Elemental *Anal.* Calc. for $C_{23}H_{27}RhN_2ClPF_6$: C, 44.93; H, 4.42; N, 4.55. Found: C, 45.56; H, 4.38; N, 4.56%.

UV–Vis (acetone): λ_{max} = 344.6 nm.

3c. Yield: 146 mg, (72%). IR (KBr pellets, cm^{-1}): $\nu_{(C=N)}$ 1596 (s), $\nu_{(P-F)}$ 840 (s).

^{1}H NMR (acetone-d_6, δ): 1.55 (s, 15H, C_5Me_5), 3.89 (s, 3H, CH_3), 7.17 (d, 2H, J_{H-H} = 4.55 Hz), 7.79 (d, 2H, J_{H-H} = 4.48 Hz), 7.99 (td, 2H, J_{H-H} = 2.14 Hz, 5.22 Hz), 8.37 (d, 1H, J_{H-H} = 7.36 Hz), 8.66 (d, 1H, J_{H-H} = 2.79 Hz), 9.15 (d, 1H, J_{H-H} = 5.29 Hz).

^{13}C NMR (acetone-d_6, δ): 8.80 (CH_3, C_5Me_5), 56.08 (CH_3), 96.35 (C, C_5Me_5), 115.35, 118.38, 122.46, 124.96 (Ph), 126.24, 127.37, 130.44, 141.27, 153.56 (py), 166.36 (C–H).

Elemental *Anal.* Calc. for $C_{23}H_{27}RhN_2OClPF_6$: C, 43.79; H, 4.31; N, 4.44. Found: C, 43.36; H, 4.36; N, 4.53%.

UV–Vis (acetone): λ_{max} = 363.6 nm.

3d. Yield: 161 mg, (79%). IR (KBr pellets, cm^{-1}): $\nu_{(C=N)}$ 1600 (s), $\nu_{(B-F)}$ 1056 (s).

^{1}H NMR ($CDCl_3$, δ): 1.82 (s, 15H, C_5Me_5), 7.52 (d, 2H, J_{H-H} = 8.68 Hz, Ph), 7.89 (d, 2H, J_{H-H} = 8.64 Hz, Ph), 8.14 (td, 1H, J_{H-H} = 9.04 Hz, 7.68 = Hz, py), 8.24 (d, 2H, J_{H-H} = 7.28 Hz, py), 8.58 (d, 1H, J_{H-H} = 2.76 Hz, imine C–H), 8.74 (d, 1H, J_{H-H} = 5.76 Hz, py).

^{13}C NMR ($CDCl_3$, δ): 8.57 (CH_3, C_5Me_5), 90.17 (C, C_5Me_5), 121.32, 126.26, 130.38, 132.47 (Ph), 135.58, 139.24, 145.31, 149.27, 155.51 (py), 164.73 (C–H).

Elemental *Anal*. Calc. for $C_{22}H_{24}RhN_2Cl_2PF_6$: C, 41.66; H, 3.81; N, 4.41. Found: C, 41.34; H, 3.47; N, 4.26%.

UV–Vis (acetone): λ_{max} = 372.5 nm.

3e. Yield 153 mg, (73%). IR (KBr pellets, cm^{-1}): $\nu_{(C=N)}$ 1593 (s), $\nu_{(NO_2,\,asymmetric)}$ 1527 (s), $\nu_{(NO_2,\,symmetric)}$ 1348 (s), $\nu_{(P-F)}$ 837 (s).

^{1}H NMR (acetone-d_6, δ): 1.47 (s, 15H, C_5Me_5), 8.06 (m, 3H, py), 8.43 (d, 2H, J_{H-H} = 8.63 Hz, Ph), 8.54 (d, 2H, J_{H-H} = 8.91 Hz), 9.07 (d, 1H, J_{H-H} = 2.80 Hz, CH), 9.24 (d, 1H, J_{H-H} = 5.36 Hz, α proton of py).

^{13}C NMR (acetone-d_6, δ): 8.84 (CH_3, C_5Me_5), 90.34 (C, C_5Me_5), 98.46, 106.54, 115.68, 124.55 (Ph), 125.92, 131.16, 131.62, 141.29, 153.57 (py), 169.84 (C–H).

Elemental *Anal*. Calc. for $C_{22}H_{24}RhN_3O_2ClPF_6$: C, 40.92; H, 3.74; N, 6.50. Found: C, 39.48; H, 3.88; N, 6.08%.

UV–Vis (acetone): λ_{max} = 369.4 nm.

*2.4. Synthesis of [(η^5-C_5Me_5)IrCl(C_5H_5N-2-CH=N–C_6H_4-p-X)]$^+$ (**4a-e**), (X = H (**4a**), CH_3 (**4b**), OCH_3 (**4c**), Cl (**4d**), NO_2 (**4e**)*

These complexes were prepared by the same method given in Section 2.3 using [{(η^5-C_5Me_5)Ir(μ-Cl)Cl}$_2$] (**2**) instead of complex [{(η^5-C_5Me_5)Rh(μ-Cl)Cl}$_2$] (**1**).

4a. Yield: 136 mg, (79%). IR (KBr pellets, cm^{-1}): $\nu_{(C=N)}$ 1600 (s), $\nu_{(P-F)}$ 844 (s).

^{1}H NMR (acetone-d_6, δ): 1.55 (s, 15H, C_5Me_5), 7.55–7.61 (m, 3H, Ph), 7.80 (d, 2H, J_{H-H} = 7.95 Hz, Ph), 7.99–8.40 (m, 3H, py), 9.19 (d, 1H, J_{H-H} = 5.05 Hz, α proton of py), 9.35 (s, 1H, CH).

^{13}C NMR (acetone-d_6, δ): 8.51 (CH_3, C_5Me_5), 91.22 (C, C_5Me_5), 123.57, 130.47, 130.90, 131.42 (Ph), 136.32, 138.47, 141.51,153.24, 157.83 (py), 169.43 (imine C–H).

Elemental *Anal*. Calc. for $C_{22}H_{25}IrN_2ClPF_6$: C, 38.29; H, 3.65; N, 4.06. Found: C, 38.47; H, 3.32; N, 4.12%.

UV–Vis (acetone): λ_{max} = 385.7 nm.

4b. Yield: 112 mg, (63%). IR (KBr pellets, cm^{-1}): $\nu_{(C=N)}$ 1633 (s), $\nu_{(P-F)}$ 844 (s).

^{1}H NMR (acetone-d_6, δ): 1.55 (s, 15H, C_5Me_5), 2.47 (s, 3H, CH_3), 7.48 (d, 2H, J_{H-H} = 8.14 Hz, Ph), 7.70 (d, 2H, J_{H-H} = 8.31 Hz, Ph), 8.00–8.03 (m, 1H, py), 8.35–8.40 (m, 2H, py), 8.51 (d 1H, J_{H-H} = 7.39 Hz, imine C–H), 9.18 (d, 1H, J_{H-H} = 5.39 Hz, α proton of py).

^{13}C NMR (acetone-d_6, δ): 8.54 (CH_3, C_5Me_5), 21.16 (CH_3), 91.17 (C, C_5Me_5), 123.49, 128.36, 130.71, 131.26 (Ph), 141.50, 148.23, 152.54, 153.20, 155.21 (py), 166.76 (imine C–H).

Elemental *Anal*. Calc. for $C_{23}H_{27}IrN_2ClPF_6$: C, 39.23; H, 3.86; N, 3.97. Found: C, 40.32; H, 3.83; N, 4.04%.

UV–Vis (acetone): λ_{max} = 385.75 nm.

4c. Yield: 133 mg, (73%). IR (KBr pellets, cm^{-1}): $\nu_{(C=N)}$ 1606 (s), $\nu_{(P-F)}$ 844 (s).

^{1}H NMR (acetone-d_6, δ): 1.57 (s, 15H, C_5Me_5), 3.76 (s, 3H, CH_3), 7.23 (d, 2H, J_{H-H} = 6.23 Hz, Ph), 7.62 (d, 2H, J_{H-H} = 6.23 Hz, Ph), 7.86–8.34 (m, 3H, py), 8.58 (d, 1H, J_{H-H} = 3.06 Hz, α proton of py), 9.23 (1H, J_{H-H} = 4.66 Hz, imine C–H).

^{13}C NMR (acetone-d_6, δ): 7.57 (CH_3, C_5Me_5), 55.15 (CH_3), 90.12 (C, C_5Me_5), 114.35, 114.60, 124.14, 129.43 (Ph), 130.10, 140.45, 148.32, 149.69, 152.15 (py), 166.64 (imine C–H).

Elemental *Anal*. Calc. for $C_{23}H_{27}IrN_2OClPF_6$: C, 38.36; H, 3.77; N, 3.89. Found: C, 38.06; H, 3.46; N, 3.95%.

UV–Vis (acetone): λ_{max} = 368.23 nm.

4d. Yield: 128 mg, (71%). IR (KBr pellets, cm^{-1}): $\nu_{(C=N)}$ 1633 (s), $\nu_{(P-F)}$ 844 (s).

^{1}H NMR (acetone-d_6, δ): 1.56 (s, 15H, C_5Me_5), 7.73 (d, 2H, J_{H-H} = 8.55 Hz, Ph), 7.65 (d, 2H, J_{H-H} = 8.81 Hz, Ph), 8.01–8.06 (m, 3H, py), 8.95 (d, 1H, J_{H-H} = 2.74 Hz, imine C–H), 9.21 (d, 1H, J_{H-H} = 5.39 Hz, α proton-py).

^{13}C NMR (acetone-d_6, δ): 7.57 (CH_3, C_5Me_5), 90.28 (C, C_5Me_5), 124.35, 129.56, 130.12, 130.58 (Ph), 140.56, 142.63, 147.34, 149.52, 152.28 (py), 169.08 (imine C–H).

Elemental *Anal*. Calc. for $C_{22}H_{24}IrN_2Cl_2PF_6$: C, 36.52; H, 3.34; N, 3.87. Found: C, 36.61; H, 3.08; N, 3.66%.

UV–Vis (acetone): λ_{max} = 385.75 nm.

4e. Yield: 132 mg, (72%). IR (KBr pellets, cm^{-1}): $\nu_{(C=N)}$ 1593 (s), $\nu_{(NO_2,\,asymmetric)}$ 1527 (s), $\nu_{(NO_2,\,symmetric)}$ 1348 (s), $\nu_{(P-F)}$ 844 (s).

^{1}H NMR (acetone-d_6, δ): 1.59 (s, 15H, C_5Me_5), 8.05–8.10 (m, 2H, py), 8.41 (d, 2H, J_{H-H} = 1.41 Hz, Ph), 8.54–8.61 (m, 1H, py), 9.26 (d, 1H, J_{H-H} = 5.5 Hz, α proton-py), 9.54 (s, 1H, imine C–H).

^{13}C NMR (acetone-d_6, δ): 8.39 (CH_3, C_5Me_5), 91.25 (C, C_5Me_5), 124.77, 125.91, 131.55, 131.77 (Ph), 141.45, 149.36, 153.20, 154.26, 156.54 (py), 171.26 (imine C–H).

Elemental *Anal*. Calc. for $C_{22}H_{24}IrN_3O_2ClPF_6$: C, 35.94; H, 3.29; N, 5.71. Found: C, 35.76; H, 3.43; N, 5.92%.

UV–Vis (acetone): λ_{max} = 387.13 nm.

3. Crystallographic investigations

Crystals suitable for X-ray diffraction study for compound **3d**[BF_4] were grown by slow diffusion of hexane

into an acetonitrile solution of **3d**[BF_4], and for compound **4e**[PF_6] by slow diffusion of hexane into a dichloromethane solution of **4e**[PF_6]. The orange crystals of compounds **3d**[BF_4] and **4e**[PF_6] were mounted on a Bruker Apex CCD diffractometer in a full reciprocal sphere equipped with a CCD detector, and were used for data collection. X-ray intensity data were collected with graphite monochromated Mo Kα radiation at 293(2) K, with 0.3° ω scan mode and 10 s per frame. The intensity data were corrected for Lorentz and polarization effects. Absorption corrections were done using the SAINT program [17]. A summary of the crystal data, data collection parameters and convergence results is compiled in Table 1. An empirical absorption correction was made by modelling a transmission surface by spherical harmonics employing equivalent reflections with $I > 2\sigma(I)$ (program SADABS) [18]. The structures were solved by direct methods [19]. All the non-hydrogen atoms were refined anisotropically using the full-matrix, least-squares technique on F^2 using the SHELXL-97 software [20]. All the hydrogen atoms were found from difference Fourier synthesis after four cycles of an isotropic refinement and as per the ''riding'' model. Figs. 3 and 4 display the ORTEP [21] representations of the molecules with 50% probability thermal ellipsoids. Refinement converged at final R_1 values of 0.0366 and 0.0313 (for observed data F) for compounds **3d**[BF_4] and **4e**[PF_6], respectively.

Table 1
Crystal data and structure refinement parameters for complexes **3d**[BF_4] and **4e**[PF_6]

Formula	$C_{22}H_{24}BCl_2F_4N_2Rh$	$C_{22}H_{24}ClF_6IrN_3O_2P$
M_r	577.05	735.06
T (K)	293(2)	293(2)
Wavelength (Å)	0.71073	0.71073
Crystal system	monoclinic	monoclinic
Space group	$P2_1/n$	$P2_1/n$
a (Å)	10.1944(6)	10.4116(6)
b (Å)	11.6110(6)	11.5786(6)
c (Å)	20.4223(11)	21.7809(12)
β (°)	96.334(10)	98.097(10)
V (Å^3)	2402.6(2)	2599.5(2)
Z	4	4
Crystal size (mm^3)	$0.45 \times 0.27 \times 0.25$	$0.15 \times 0.28 \times 0.35$
D_{calc} (g cm^{-3})	1.595	1.878
$F(000)$	1160	1424
θ (°)	2.01–28.30	1.89–28.30
Reflections collected	20524	22158
Independent reflections [R_{int}]	5645 [0.0180]	6119 [0.0285]
Absorption coefficient (mm^{-1})	0.977	5.368
Completeness to θ (°)	28.30	28.30
Data/restraints/parameters	5645/0/255	6119/0/297
Goodness-of-fit on F^2	1.046	1.059
R_1 ($I > 2\sigma(I)$), wR_2	0.0366, 0.1062	0.0313, 0.0812
R_1, R_2 (all data)	0.0410, 0.1100	0.0417, 0.0863
Largest difference in peak and hole (e Å^{-3})	+0.804 and −0.617	+2.159 and −0.616

4. Results and discussion

The dinuclear complexes [{(η^5-C_5Me_5)M(μ-Cl)Cl}$_2$] {M = Rh (**1**) and Ir (**2**)} undergo a bridge cleavage reaction with *N*,*N*′-donor Schiff base ligands (**2-PP**) in methanol to yield cationic complexes **3** and **4** (Scheme 1), respectively. These complexes are isolated as the hexafluorophosphate salts. The orange-yellow complexes are air-stable microcrystalline solids, partially soluble in chloroform, methanol and benzene, soluble in dichloromethane, acetone and insoluble in hexane, petroleum ether and diethyl ether.

The infrared spectra of these complexes show a strong band in the range 1593–1633 cm^{-1} due to the $\nu_{C=N}$ group of the Schiff base ligand, and a strong band in the range 837–844 cm^{-1} due to the ν_{P-F} mode of the PF_6^- group. The complexes **3e** and **4e** exhibit the characteristic bands for ν_{NO_2} (asymmetric stretch at 1527 cm^{-1} and symmetric stretch at 1346 cm^{-1}). The ^{1}H NMR spectral data of these complexes along with their assignments are recorded in the experimental section. In the ^{1}H NMR spectra of these complexes, the methyl group of the pentamethylcyclopentadienyl protons appears as a singlet in the range 1.47–1.82 ppm, which are shifted downfield as compared to that in the precursor complexes. A downfield shift in the position of the Cp* protons might result from the change in electron density on the metal center due to chelation of the Schiff base ligands through their nitrogen atoms. The multiplet observed in the range 7.32–8.61 ppm is due to the phenyl protons of the amine group and the *N*-heterocyclic ring of the ligands (**2-PP**), these resonance values being consistent with the reported values [8]. The ^{13}C {^{1}H} NMR spectra of complexes **3** and **4** exhibit resonances for the methyl carbons of the pentamethylcyclopentadienyl group at around 8.00 ppm and for the ring carbons at around 90.12–98.37 ppm. The resonance observed in the range 158.56–171.26 ppm is assigned to the imine group of the ligand (**2-PP**). The spectra also show resonances in the range 98.46–157.83 ppm for the aromatic carbon of the phenyl group and pyridyl group carbons (see Fig. 1).

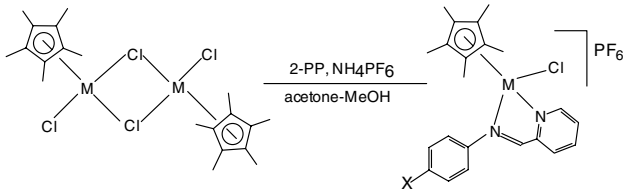

M = Rh(1) Ir(2)

2-PP = N-(pyrid-2-ylmethelene)phenylamine

M = Rh; X = H(3a)
CH_3(3b)
OCH_3(3c)
Cl(3d)
NO_2(3e)

M = Ir X = H(4a)
CH_3(4b)
OCH_3(4c)
Cl(4d)
NO_2(4e)

Scheme 1.

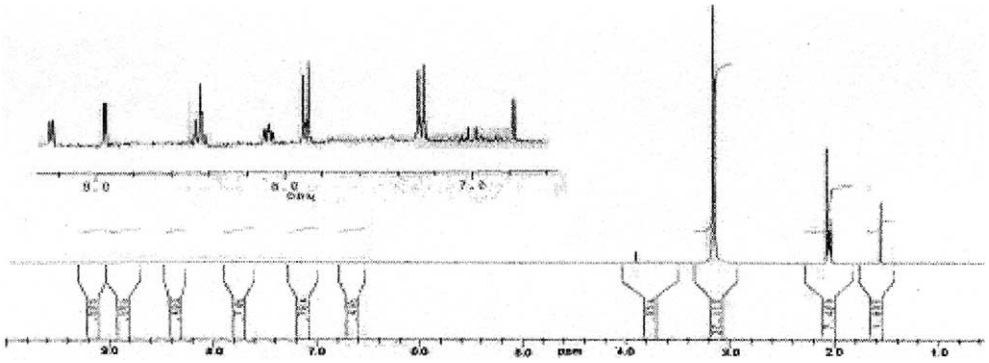

Fig. 1. ^{1}H NMR spectrum of complex $[(\eta^5\text{-}C_5Me_5)RhCl(C_5H_4N\text{-}2\text{-}CH{=}N\text{–}C_6H_4\text{-}p\text{-}OMe)]^+$ (**3c**) in acetone-d_6.

The electronic absorption spectra for rhodium (III) and iridium (III) Schiff base complexes typically contains π–π* and *n*–π* bands in the ultraviolet region The interaction of the filled dπ (t_2g) orbitals on rhodium (III) and iridium (III) with low lying π* orbitals on the Schiff base imine (C=N) ligands should provide a metal-to-ligand charge transfer (MLCT) transition (t_2g-π*) in the electronic spectra of these complexes [22–24] with the transition energy of these bands varying with the nature of the ligands acting as π-acceptors. The electronic spectra of these complexes in acetone exhibit bands in the range of 344–387 nm. This low-energy absorption is assigned to a Rh dπ (or Ir dπ) to ligand π* metal-to-ligand charge transfer (MLCT) transition (see Fig. 2).

Electron transfer properties of the representative compound **3a**[PF_6] are studied in acetonitrile solvent by cyclic voltametry. The first reduction wave of this rhodium (III) complex occurs at around −0.544 V and the corresponding oxidation wave at −0.113 V; it shows a quasi-reversible plot (ΔE = −431 mV). This is assigned to the Rh(III)/Rh(II) couple [Eq. (1)]. The second reduction wave occurs at −1.199 V and the corresponding oxidation wave −0.824 V; this also shows a quasi-reversible plot (ΔE = −375 mV), which is a two-electron transfer Rh(III)/Rh(I) couple. We have also observed here the Rh(III)/Rh(II) and Rh(II)/Rh(I) couple.

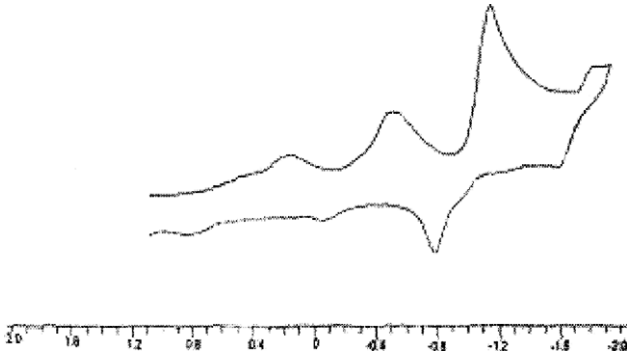

Fig. 2. Cyclic voltammogram of complex $[(\eta^5\text{-}C_5Me_5)RhCl(C_5H_4N\text{-}2\text{-}CH{=}N\text{–}C_6H_5)]^+$ (**3a**) in acetonitrile using a Pt-disk milli electrode at 298 K, SCE reference and TBAP (0.1 M) supporting electrolyte.

$$[(\eta^5 - C_5Me_5)RhCl(2 - PP)]^+ + e^- \leftrightarrows [(\eta^5 - C_5Me_5)RhCl(2 - PP)] \quad (1)$$

In general, ligand effects appear in the Ru(IV/III) and Ru(III/II) redox potentials. Ligand effects on the Ru(III/II) couple are well known, where Ru(III/II) potentials are influenced along with the ligand. Ru(II) is stabilized by the contribution of dπ–π* (L) back bonding in the presence of the ligands. The replacement of a Schiff-base ligand by the strongly electron-donating pentamethylcyclopentadienyl group destabilizes the lower rhodium oxidation states, making reduction more difficult. Indeed, in our observation the reduction potential for the +3/+1 couple of $[Cp^*RhCl(2\text{-}PP)]^+$ falling may arise from the intermediate $[Rh(Cp^*)_2]^+$ and $[Rh(2\text{-}PP)_3]^{3+}$.

5. Molecular structures

Single crystal X-ray structure determinations were carried out for compounds **3d** and **4e** for confirmation of their formulae and structure. The rhodium atom compound **3d** and the iridium atom compound **4e** are coordinated to two nitrogen atoms of the Schiff base (**2-PP**) ligand, one chloride ion and the pentamethylcyclopentadienyl molecule in a η^5-fashion leading to the usual 'three-legged piano stool' structures. The geometry around the metal atom can be regarded as distorted octahedral if the η^5-pentamethylcyclopentadienyl moieties are assumed to occupy three facial-coordinated positions. A summary of the single-crystal X-ray structure analyses is shown in Table 1. Selected bond lengths and bond angles are given in Tables 2 and 3. The ORTEP drawings of compounds **3d** and **4e** are shown in Figs. 3 and 4, respectively.

The tetrafluoroborate salt of complex $[(\eta^5\text{-}C_5Me_5)RhCl(C_5H_4N\text{-}2\text{-}CH{=}N\text{–}C_6H_4\text{-}p\text{-}Cl)]^+$**3d** and hexafluorophosphate salt of complex $[(\eta^5\text{-}C_5Me_5)IrCl(C_5H_4N\text{-}2\text{-}CH{=}N\text{–}C_6H_4\text{-}p\text{-}NO_2)]^+$ **4e** crystallize in the monoclinic space group $P2_1/n$ (Figs. 3 and 4). The two metal-centroid distances are indistinguishable (1.791 Å). The bond distances between the rhodium and iridium metal

Table 2
Selected bond lengths (Å) and bond angles (°) for $[(\eta^5\text{-}C_5Me_5)RhCl(C_5H_4N\text{–}2CH{=}N\text{–}C_6H_4\text{-}p\text{-}Cl)]^+$ (**3d**)

Bond lengths (Å)	
Rh–N	2.123(2)
N–C(21)	1.422(2)
N(32)–C(31)	1.3900
Rh–N(32)	2.0949(11)
N–C	1.271(4)
Rh–C[a]	1.791
Rh–Cl(1)	2.3756(7)
N(32)–C(33)	1.3900
Bond angles (°)	
N(32)–Rh–N	76.17(7)
N(32)–Rh–Cl(1)	85.13(4)
N–Rh–Cl(1)	86.76(6)

[a] Rhodium to centroid of Cp*.

Table 3
Selected bond lengths (Å) and bond angles (°) for $[(\eta^5\text{-}C_5Me_5)IrCl(C_5H_4N\text{-}2\text{-}CH{=}N\text{–}C_6H_4\text{-}p\text{-}NO_2)]^+$ (**4e**)

Bond lengths (Å)	
Ir–N(1)	2.099(4)
N(21)–C(26)	1.3900
N(1)–C(1)	1.285(5)
Ir–C[a]	1.792
Ir–Cl	2.3726(11)
N(21)–C(22)	1.3900
N(2)–O(1)	1.198(8)
Ir–N(21)	2.0862(18)
N(1)–C(31)	1.408(4)
N(2)–O(2)	1.171(8)
Bond angles (°)	
N(21)–Ir–Cl	84.45(8)
N(1)–Ir–Cl	85.17(9)
N(21)–Ir–N(1)	75.98(11)

[a] Iridium to centroid of Cp*.

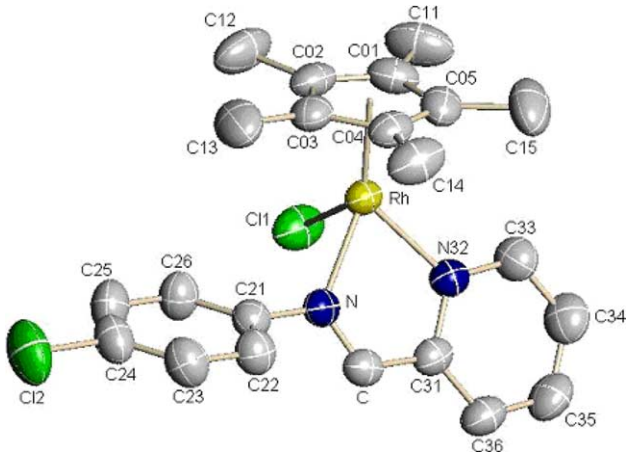

Fig. 3. ORTEP representation of the complex **3d** with 50% probability thermal ellipsoids. Hydrogens and BF_4^- are omitted for clarity.

atoms and the chelated ligand nitrogen atoms are similar to each other (~2.1 Å). There is no significant difference in the C–C bond lengths in the pentamethylcyclopentadienyl ring, all being about 1.42

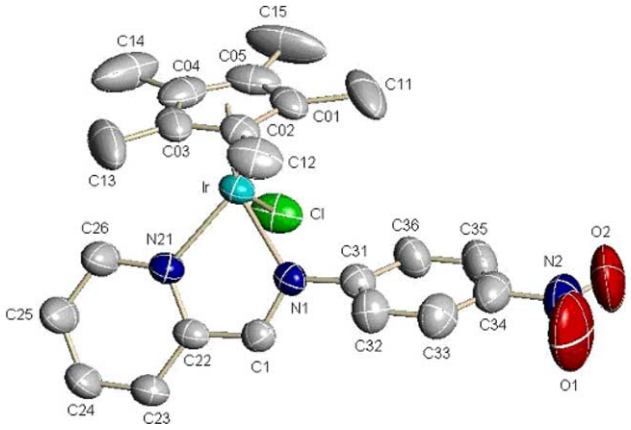

Fig. 4. ORTEP representation of the complex **4e** with 50% probability thermal ellipsoids. Hydrogens and PF_6^- are omitted for clarity.

Å and pointing to π-electron delocalization in the ring. Furthermore, the five membered ring is planar as evident in the nearly equal bond distances between metal atom and the ring carbons. The Rh–Cl and Ir–Cl bond distances are 2.3756(7) and 2.3726(11) Å, respectively, which are closely similar to another related two-coordinated chelating polypyridyl rhodium complex $[Cp^*RhCl(Phterpy)]^+$ (2.3984(1)) [25].

6. Concluding remarks

We have observed interesting phenomena in the case of the pentamethylcyclopentadienyl compounds of **1** and **2**, which distinguish them from the analogous pentamethylcyclopentadienyl or indenyl ruthenium (II) systems, even though these are all isoelectronic. Unlike in the case of the compounds **1** and **2**, the reactions of Schiff bases with the $[(\eta^5\text{-}Cp^*)Ru(PPh_3)_2Cl]$ and $[(\eta^5\text{-ind.})Ru(PPh_3)_2Cl]$ systems yielded complexes without any organic group. In order to obtain similar complexes for these cases, one has to start from the acetonitrile complexes.

Acknowledgements

We thank Professor R.H. Duncan Lyngdoh for his help in preparing the manuscript and Dr. A. Lemtur for helpful discussions in the electrochemistry part.

Appendix A. Supplementary data

Crystallographic data (excluding structure factors) for the structures reported in this paper have been deposited with the Cambridge Crystallographic Data Centre as supplementary publication No. CCDC 265789 for complex **3d**[BF_4] and CCDC 265788 for

complex **4e**[PF_6]. Copies of the data can be obtained free of charge on application to CCDC, 12 Union Road, Cambridge CB2 1EZ, UK (fax: Int. code +(44) 1223/336033; e-mail: deposit@ccdc.cam.ac.uk or http://www.ccdc.cam.ac.uk). Supplementary data associated with this article can be found, in the online version at doi:10.1016/j.poly.2005.04.034.

References

[1] H. Brunner, Adv. Organomet. Chem. 18 (1980) 151.
[2] S.G. Davies, Pure Appl. Chem. 60 (1988) 13.
[3] J.W. Faller, M.R. Mazzieri, J.T. Nguyen, P. Parr, M. Tokunaga, Pure Appl. Chem. 66 (1994) 1463.
[4] E.P. Kundig, A. Quettropani, M. Inage, A. Ripa, C. Dupre, A.F.J. Cunningham, B. Bourdin, Pure Appl. Chem. 68 (1996) 97.
[5] R. Noyori, S. Hashiguchi, Acc. Chem. Res. 30 (1997) 97, and references therein.
[6] V.I. Sokolov, Chirality and Optical Activity in Organometallic Compounds, Gordon and Breach, 1990.
[7] G. Consiglio, F. Morandini, Chem. Rev. 87 (1987) 761.
[8] (a) P. Govindaswamy, Y.A. Mozharivskyj, M.R. Kollipara, Polyhedron 23 (2004) 1567;
(b) R. Lalrempuia, M.R. Kollipara, P.J. Carroll, Polyhedron 22 (2003) 605;
(c) S.S. Keisham, Y.A. Mozharivskyj, P.J. Carroll, M.R. Kollipara, J. Organomet. Chem. 689 (2004) 1249.
[9] R. Lalrempuia, P. Govindaswamy, Y.A. Mozharivskyj, M.R. Kollipara, Polyhedron 23 (2004) 1069.
[10] M.R. Kollipara, E.K. Rymmai, Polyhedron 22 (2003) 307.
[11] (a) P. Govindaswamy, Y.A. Mozharivskyj, M.R. Kollipara, J. Organomet. Chem. 689 (2004) 3265;
(b) P. Govindaswamy, H.P. Yennawar, M.R. Kollipara, J. Organomet. Chem. 689 (2004) 3108;
(c) P. Govindaswamy, P.J. Carroll, Y.A. Mozharivskyj, M.R. Kollipara, J. Organomet. Chem. 690 (2005) 885;
(d) P. Govindaswamy, Y.A. Mozharivskyj, M.R. Kollipara, Polyhedron 23 (2004) 3115.
[12] (a) D.L. Davies, J. Fawcett, R. Krafczyk, D.R. Russell, J. Organomet. Chem. 545–546 (1997) 581;
(b) S.K. Mandal, A.R. Chakravarty, Polyhedron 10 (1991) 2483.
[13] S. Pal, T.K. Misra, C. Sinha, A.M.Z. Slawin, J.D. Woolins, Polyhedron 19 (2000) 1925.
[14] (a) R.N. Dominey, B. Hauser, J. Habbard, J. Dunham, Inorg. Chem. 30 (1991) 4754;
(b) E.V. Dose, L.J. Wilson, Inorg. Chem. 17 (1978) 2660.
[15] (a) J.W. Kang, K. Moseley, P.M. Maitlis, J. Am. Chem. Soc. 91 (1969) 5970;
(b) R.G. Ball, W.A.G. Graham, D.M. Heinekey, J.K. Hoyano, A.D. McMaster, B.M. Mattson, S.T. Michel, Inorg. Chem. 29 (1990) 2023;
(c) C. White, A. Yates, P.M. Maitlis, Inorg. Synth. 29 (1992) 228.
[16] P. Byabartta, J. Dinda, P.K. Santra, C. Sinha, K. Panneerselvam, F.-L. Liao, T.-H. Lu, J. Chem. Soc., Dalton Trans. (2001) 2825.
[17] D. Becke, J. Chem. Phys. 98 (1993) 5648.
[18] XRD Single Crystal Software; Bruker Analytical X-ray Systems, Madison, USA, 2002.
[19] G.M. Sheldrick, SHELXS86, Program for Crystal Structure Solution, University of Göttengen, Göttengen, Germany, 1986.
[20] M. Sheldrick, SHELXS97, Program for Crystal Structure Refinement, University of Göttengen, Göttengen, Germany, 1997.
[21] C.K. Johnson, ORTEP – II: A Fortran Thermal Ellipsoid Plot Program for Crystal Structure Illustrations, ORNL – 5138, 1976.
[22] B.K. Ghosh, A. Chakravorty, Coord. Chem. Rev. 95 (1989) 239.
[23] (a) N. Bag, G.K. Lahiri, A. Chakravorty, Inorg. Chem. 31 (1992) 40;
(b) G.K. Lahiri, S. Bhattacharya, S. Goswami, A. Chakravorty, J. Chem. Soc., Dalton Trans. (1990) 561;
(c) G.K. Lahiri, S. Goswami, L.R. Falvello, A. Chakravorty, Inorg. Chem. 26 (1987) 3365;
(d) P. Ghosh, A. Chakravorty, J. Chem. Soc., Dalton Trans. (1985) 361.
[24] (a) T.K. Misra, D. Das, C. Sinha, P.K. Ghosh, C.K. Pal, Inorg. Chem. 37 (1998) 1672;
(b) P. Byabartta, S.K. Jasimuddin, B.K. Ghosh, C. Sinha, A.M.Z. Slawin, J.W. Woollins, New J. Chem. 26 (2002) 1415;
(c) J. Dinda, D. Das, P.K. Santra, C. Sinha, L.R. Falvello, J. Organomet. Chem. 629 (2001) 28;
(d) J. Dinda, S.K. Jasimuddin, G. Mostafa, C.-H. Hung, C. Sinha, Polyhedron 23 (2004) 793;
(e) S. Pal, D. Das, C. Sinha, C.H.L. Kennard, Inorg. Chim. Acta 313 (2001) 21.
[25] H. Aneetha, P.S. Zacharias, B. Srinivas, G.H. Lee, Y. Wang, Polyhedron 18 (1999) 299.